Exact one- and two-particle excitation spectra of acute-angle helimagnets above their saturation magnetic field

R. O. Kuzian
Institute for Problems of Materials Science Krzhizhanovskogo 3, 03180 Kiev, Ukraine

S.-L. Drechsler
Leibniz-Institut für Festkörper- und Werkstofforschung IFW Dresden, P.O. Box 270116, D-01171 Dresden, Germany

(Received 24 April 2006; revised manuscript received 23 October 2006; published 2 January 2007)

The two-magnon problem for the frustrated XXZ spin-1/2 Heisenberg Hamiltonian and external magnetic fields exceeding the saturation field B_s is considered. We show that the problem can be *exactly* mapped onto an effective tight-binding impurity problem. It allows to obtain explicit exact expressions for the two-magnon Green's functions *for arbitrary dimension and number of interactions*. We apply this theory to a quasi-one-dimensional helimagnet with ferromagnetic nearest-neighbor $J_1<0$ and antiferromagnetic next-nearest neighbor $J_2>0$ interactions. An outstanding feature of the excitation spectrum is the existence of two-magnon bound states. This leads to deviations of the saturation field B_s from its classical value B_s^{cl} which coincides with the one-magnon instability. For the refined frustration ratio $|J_2/J_1|>0.374\,661$ the minimum of the two-magnon spectrum occurs at the boundary of the Brillouin zone. Based on the two-magnon approach, we propose general analytic expressions for the saturation field B_s, confirming known previous results for one-dimensional isotropic systems, but explore also the role of interchain and long-ranged intrachain interactions as well as of the exchange anisotropy.

DOI: 10.1103/PhysRevB.75.024401 PACS number(s): 75.30.Ds, 75.30.Gw, 75.10.Pq, 75.10.Jm

I. INTRODUCTION

We study a spin-1/2 quasi-one-dimensional helimagnet with ferromagnetic ($J_1<0$) nearest-neighbor and antiferromagnetic ($J_2>0, |J_2/J_1|>1/4$) next-nearest-neighbor in-chain interactions. In the classical approximation the spins are vectors. In zero magnetic field, they form a planar spiral structure (say in the xy plane) with a pitch angle

$$\cos\varphi^{\mathrm{cl}} = -J_1/4J_2$$

between neighboring spins. When a magnetic field is applied along the z axis, the spin moments are inclined toward the z axis by an angle

$$\sin\theta^{\mathrm{cl}} = 8\mu B J_2/(4J_2+J_1)^2,$$

where $\mu=-g\mu_B$ is the value of the magnetic moment. For fields greater than

$$\mu B_s^{\mathrm{cl}} = (4J_2+J_1)^2/8J_2 \tag{1}$$

the angle $\theta=\pi/2$ and the system becomes "ferromagnetic" (fully polarized uniform state).

In the quantum case, this high-field ferromagnetic state becomes unstable when the frequency of a certain excitation mode vanishes. The one-particle instability occurs just at the classical field B_s^{cl} given by Eq. (1). For the collinear antiferromagnet and the obtuse-angle helimagnet ($\varphi>\pi/2$) the quantum saturation field coincides with the classical one.[1] In contrast, for an acute-angle helimagnet ($\varphi<\pi/2$) the corresponding saturation field *exceeds* the classical value B_s^{cl}[2,3] due to the existence of n-magnon bound states below the n-magnon continuum (see Sec. II B of Ref. 3).

Below we derive an explicit exact expression for the two-magnon Green's function at magnetic fields $B>B_s$. It exhibits isolated poles below the two-particle continuum which correspond to two-magnon bound states. According to Refs. 2 and 3, for $|J_2/J_1|>|\alpha_c|\approx 0.38$ the two-magnon spectrum minimum determines the saturation field $B_s>B_s^{\mathrm{cl}}$. Our approach allows to refine the value of α_c, to reproduce their results for B_s for the isotropic J_1-J_2 Heisenberg model and to generalize it to more complex situations of exchange anisotropy and interchain interaction as well as of an additional in-chain interaction J_3.

II. THE MODEL AND NOTATIONS

The Hamiltonian of the model reads

$$\hat{H} = -\mu B\sum_m \hat{S}_m^z + \frac{1}{2}\sum_{m,r}\left[J_r^z\hat{S}_m^z S_{m+r}^z + \frac{J_r^{xy}}{2}(\hat{S}_m^+\hat{S}_{m+r}^- + \hat{S}_m^-\hat{S}_{m+r}^+)\right], \tag{2}$$

where m enumerates the sites in the chain, r determines the nearest- ($r=\pm 1$) and the next-nearest- ($r=\pm 2$) neighboring sites. We have allowed for an uniaxial anisotropy of the exchange interactions. We restrict ourselves to the case of $s=1/2$. Then the model given by Eq. (2) can be applied to undoped edge-shared chain cuprates.[4] Here the spin operators $\hat{S}_m^\alpha$ may be expressed via the hard-core boson operators b_m

$$\hat{S}^+ \equiv b, \quad \hat{S}^- \equiv b^\dagger, \quad \hat{S}^z \equiv \frac{1}{2} - \hat{n}, \tag{3}$$

$$[b_m, b_{m'}^\dagger] = (1-2\hat{n}_m)\delta_{mm'}, \tag{4}$$

$$\hat{n} = b_m^\dagger b_m = 0,1, \tag{5}$$

where the square brackets stand for the commutator, and m denotes the site index. The ferromagnetic state corresponds to the vacuum state $b|\mathrm{FM}\rangle = b|0\rangle = 0$. Then the Hamiltonian (2) can be rewritten as

$$\hat{H} = \hat{H}_0 + \hat{H}_{int}, \tag{6}$$

$$\hat{H}_0 = \omega_0 \sum_m \hat{n}_m + \frac{1}{2}\sum_{m,r} J_r^{xy} b_m^\dagger b_{m+r}, \tag{7}$$

$$\omega_0 \equiv \mu B - \frac{1}{2}\sum_r J_r^z,$$

$$\hat{H}_{int} = \frac{1}{2}\sum_{m,r} J_r^z \hat{n}_m \hat{n}_{m+r}. \tag{8}$$

The transverse part of $\hat{H}$ (2) defines the one-particle hoppings in $\hat{H}_0$ (7), the Ising part contributes the interaction (8) and on-site energy value ω_0.

We shall study the one- and two-particle excitation spectra of the Hamiltonian given by Eq. (6) which will be obtained from the singularities (poles and branch cuts) of the corresponding retarded Green's functions (GF):

$$G^{(1)}(q,\omega) = \langle\langle b_q | b_q^\dagger \rangle\rangle, \tag{9}$$

$$G_{l,a}(k,\omega) = \langle\langle A_{k,l} | A_{k,a}^\dagger \rangle\rangle, \tag{10}$$

where

$$\langle\langle \hat{X} | \hat{Y} \rangle\rangle \equiv -i\int_{t'}^{\infty} dt e^{i\omega(t-t')} \langle [\hat{X}(t), \hat{Y}(t')] \rangle,$$

$$\hat{A}_{k,l} \equiv \frac{1}{\sqrt{N}}\sum_q e^{iql} b_{k/2+q} b_{k/2-q} = \frac{1}{\sqrt{N}}\sum_m e^{-ik(m+l/2)} b_m b_{m+l}. \tag{11}$$

The expectation value $\langle \cdots \rangle$ denotes the ground state average, the time dependence of an operator $\hat{X}(t)$ is given by $\hat{X}(t) = e^{it\hat{H}}\hat{X}e^{-it\hat{H}}$, and the Fourier transform of b_m reads $b_q = N^{-1/2}\Sigma_m \exp(-iqm) b_m$. N denotes the total number of sites.

III. THE ONE-MAGNON SPECTRUM

The equation of motion for the hard-core boson operators (3) reads

$$i\frac{d}{dt} b_m = [b_m, \hat{H}] = \omega_0 b_m + \sum_r \left[J_r^{xy}\left(\frac{1}{2} - \hat{n}_m\right) b_{m+r} + J_r^z \hat{n}_{m+r} b_m \right]. \tag{12}$$

For the ferromagnetic ground state, the terms proportional to $\hat{n}$ do not contribute to the one-magnon GF (9). This means that the usually infinite hierarchy of equations of motion including higher-order Green's function is cut exactly and closed rigorous expressions for all n-magnon Green's function can be obtained in principle. In particular, the one-magnon GF becomes simply

$$G^{(1)}(q,\omega) = \langle\langle b_q | b_q^\dagger \rangle\rangle = (\omega - \omega_q^{\mathrm{SW}})^{-1}, \tag{13}$$

where

$$\omega_q^{\mathrm{SW}} = \omega_0 + \frac{1}{2}\sum_r J_r^{xy} \exp(iqr) \tag{14}$$

is the free spin-wave dispersion.

The dispersion ω_q^{SW} has a minimum at the helical wave vector $q_0 = \varphi^{\mathrm{cl}}/a$, where $a=1$ is the lattice constant.

For the anisotropic Hamiltonian (2) it is convenient to define

$$\alpha \equiv J_2^{xy}/J_1^{xy}, \quad \Delta_i \equiv J_i^z/J_i^{xy}. \tag{15}$$

Then

$$\cos\varphi^{\mathrm{cl}} = -1/4\alpha, \tag{16}$$

and for magnetic fields values smaller than

$$\mu B_s^{\mathrm{cl}} = J_1^z + J_2^z + J_2^{xy} + \frac{(J_1^{xy})^2}{J_2^{xy}} = J_2^{xy}\left[\frac{\Delta_1 - 1}{\alpha} + \Delta_2 - 1 + \frac{(4\alpha+1)^2}{8\alpha^2}\right] \tag{17}$$

$\omega_{q_0}^{\mathrm{SW}}$ becomes negative. Evidently, in the isotropic case $\Delta_1 = \Delta_2 = 1$, Eq. (17) reduces to Eq. (1).

IV. THE TWO-MAGNON GREEN'S FUNCTION

The operator $\hat{A}_{k,l}$ (11) annihilates a pair of particles, separated by the distance l and moving with total quasimomentum k. A two-particle bound state manifests itself by an isolated pole of the two-magnon GF (TMGF) (10). The hard-core condition (5) demands $\hat{A}_{k,0} \equiv 0$. We see also from Eq. (11) that $\hat{A}_{k,l} = \hat{A}_{k,-l}$. The time evolution of $\hat{A}_{k,l}$, $l>0$ is given by the relation

$$i\frac{d}{dt}\hat{A}_{k,l} = [\hat{A}_{k,l}, \hat{H}] = 2\omega_0 \hat{A}_{k,l} + \frac{1}{\sqrt{N}}\sum_m e^{-ik(m+l/2)} \times \left\{ \sum_r \left[J_r^{xy}\left(\frac{1}{2} - \hat{n}_m\right) b_{m+r} + J_r^z \hat{n}_{m+r} b_m \right] b_{m+l} + \hat{A}'_{m,l} \right\}, \tag{18}$$

$$\hat{A}'_{m,l} \equiv \sum_r b_m \left[J_r^{xy}\left(\frac{1}{2} - \hat{n}_{m+l}\right) b_{m+l+r} + J_r^z \hat{n}_{m+l+r} b_{m+l} \right]. \tag{19}$$

Using the commutation relations (4), and the symmetry $J_{-r} = J_r$ we rewrite the operator $\hat{A}'_{k,l}$ in the normal form

$$\hat{A}'_{m,l} = \sum_r \left[J_r^{xy} \left(\frac{1}{2} - \hat{n}_{m+l} \right) b_m b_{m+l+r} + J_r^z \hat{n}_{m+l+r} b_m b_{m+l} \right] + \sum_r \left[-\delta_{l,0} J_r^{xy} b_m b_{m+l+r} + \delta_{l,r} J_r^z b_m b_{m+l} \right].$$

Again we note that for the ferromagnetic ground state, the terms containing the operators $\hat{n}$ do not contribute to the GF and as discussed in the previous section corresponding higher-order GF vanish exactly. Then, within the subspace of two-particle excitations above the ferromagnetic ground state, we may write rigorously

$$[\hat{A}_{k,l}, \hat{H}] = (2\omega_0 + J_l^z)\hat{A}_{k,l} + (1 - \delta_{l,0}) \sum_r J_r^{xy} \cos \frac{kr}{2} \hat{A}_{k,l+r}. \tag{20}$$

Thus, the problem of calculation of the TMGF (10) is equivalent to the impurity problem for the one-dimensional (1D) tight-binding-like Hamiltonian

$$\hat{H}_{\text{tb}}(k) = \hat{T} + \hat{V},$$

$$\hat{T} = 2\omega_0 \sum_m |m\rangle\langle m| + \sum_{m,r} |m+r\rangle t_r \langle m|,$$

$$\hat{V} = \sum_{m'} |m'\rangle \varepsilon_{m'} \langle m'|, \tag{21}$$

where

$$t_r(k) = J_r^{xy} \cos \frac{kr}{2}, \quad m' = 0, r, \quad \varepsilon_0 = \infty, \quad \varepsilon_r = J_r^z. \tag{22}$$

Let us note that the infinite value of ε_0 is the result of the hard-core constraint given by Eq. (5). The periodic part $\hat{T}$ results from $\hat{H}_0$ (7), and $\hat{H}_{int}$ (8) defines the changes of the on-site energies on impurity sites.

It is easy to see that

$$G_{l,a}(k,\omega) = \langle \phi_l | (\omega - \hat{H}_{\text{tb}})^{-1} | \phi_a \rangle, \tag{23}$$

where $|\phi_j\rangle = (|j\rangle + |-j\rangle)/\sqrt{2}$, $j = l, a$.

In a standard way, we will use the identity

$$(\omega - \hat{H}_{\text{tb}})^{-1} = (\omega - \hat{T})^{-1} + (\omega - \hat{T})^{-1} \hat{V} (\omega - \hat{H}_{\text{tb}})^{-1} \tag{24}$$

for the solution of the impurity problem in the real space. After some algebra we obtain

$$G_{1,1}(k,\omega) = \frac{1}{-J_1^z + \dfrac{1}{G_{1,1}^{(0)} + \dfrac{G_{1,2}^{(0)} J_2^z G_{2,1}^{(0)}}{1 - G_{2,2}^{(0)} J_2^z}}}, \tag{25}$$

where $G_{l,a}^{(0)}$ is the GF of noninteracting hard-core bosons ($\hat{H} = \hat{H}_0$):

$$G_{l,a}^{(0)}(k,\omega) = \langle\langle A_{k,l} | A_{k,a}^\dagger \rangle\rangle_0 = g_{l+a} + g_{l-a} - \frac{2 g_l g_a}{g_0}, \tag{26}$$

$$g_l(k,\omega) \equiv \frac{1}{N} \sum_q \frac{\cos ql}{\omega - (\omega_{k/2+q}^{\text{SW}} + \omega_{k/2-q}^{\text{SW}})}. \tag{27}$$

V. THE TWO-MAGNON BOUND STATES AND THE SATURATION FIELD

In the derivation of the exact expression for the Green's function (25)–(27) we have used the mathematical equivalence of the Heisenberg model (2) at high fields with the 1D impurity problem (21). But the obtained explicit expressions have a rather complicated form. Fortunately, the physics of the same 1D impurity problem helps also considerably in its further analysis.

The branch cut of $G_{1,1}(k,\omega)$ (25) is defined by the continuous part of the spectrum of $\hat{H}_{\text{tb}}(k)$ given by Eq. (21) that corresponds to the two-particle continuum of the starting Hamiltonian (2). Its boundaries may be found from the spectrum of the periodic part $\hat{T}$:

$$E(k,q) = 2[\omega_0 + t_1(k)\cos q + t_2(k)\cos 2q] = \omega_{k/2+q}^{\text{SW}} + \omega_{k/2-q}^{\text{SW}}.$$

Since $t_1(k) < 0$ for all k, we have

$$E(k,q_1) < E(k,q) < E(k,\pi), \quad |k| < k_1, \tag{28}$$

$$E(k,0) < E(k,q) < E(k,\pi), \quad k_1 < |k| < k_2, \tag{29}$$

$$E(k,0) < E(k,q) < E(k,q_1), \quad k_2 < |k| < \pi, \tag{30}$$

where

$$\cos q_1 = -t_1(k)/4t_2(k),$$

$$E(k,q_1) \equiv 2\omega_0 - t_1^2/4t_2 - 2t_2,$$

$$k_1 \equiv 2 \arccos \frac{\sqrt{128\alpha^2 + 1} + 1}{16|\alpha|} < \pi/2, \quad t_1(k_1)/4t_2(k_1) = -1,$$

$$k_2 \equiv 2 \arccos \frac{\sqrt{128\alpha^2 + 1} - 1}{16|\alpha|} > \pi/2, \quad t_1(k_2)/4t_2(k_2) = 1.$$

As we will see below, the point $k = \pi$ has a special meaning. For this value of k the nearest-neighbor hopping $t_1(\pi) = 0$, and the Hamiltonian $\hat{T}$ describes two noninteracting linear chains (i.e., the sites with odd or even numbers m) with a hopping $t_2(\pi) = -J_2^{xy}$ inside each chain. The account of the hard-core constraint (5), i.e., the introduction of $\hat{V}_0 = |0\rangle\varepsilon_0\langle 0|$ with $\varepsilon_0 = \infty$ entering the Hamiltonian $\hat{H}_{\text{tb}}(k)$ given by Eq. (21), does not influence the chain with odd sites, but the chain with even sites m is broken into two independent semi-infinite chains. Now, it is easy to account for the rest of terms in the impurity Hamiltonian $\hat{V}$, because $\varepsilon_1 = J_1$ and $\varepsilon_2 = J_2$ affect different chains. The GF $G_{2,2}^{(2)}(\pi,\omega)$ has a particular simple form. It can be obtained, e.g., by the recursion method

$$G_{2,2}(\pi,\omega) = [\omega - (2\omega_0 + J_2^z) - (J_2^{xy})^2 G_{2,2}^{(0)}(\pi,\omega)]^{-1}$$
$$= \frac{1}{J_2^{xy}[z - \Delta_2 - \tau(z)]}, \tag{31}$$

where the dimensionless energy

$$z \equiv (\omega - 2\omega_0)/J_2^{xy} \tag{32}$$

is introduced, and $\tau(z) \equiv (z - \sqrt{z^2-4})/2 = 1/[z - \tau(z)]$ is the local Green's function on the first site of the unperturbed semi-infinite chain in dimensionless units. A simple analysis of the expression (31) shows that besides the branch cut in the interval $-2 < z < 2$ of the real axis, $G_{2,2}(\pi,\omega)$ may have an isolated pole. The pole exists for $\Delta_2 > 1$ *above* the continuum, i.e., a bound state exists for the easy-axis anisotropy of the next-nearest-neighbor exchange. The expression for $G_{1,1}(\pi,\omega)$ is more complicated than $G_{2,2}(\pi,\omega)$:

$$G_{1,1}(\pi,\omega) = [\omega - (2\omega_0 + J_1^z - J_2^{xy}) - J_2^{xy}\tau(z)]^{-1} \tag{33}$$

$$= \frac{1}{J_2^{xy}[z - \Delta_1/\alpha + 1 - \tau(z)]}. \tag{34}$$

Note that for any acute-angle helimagnet ($\alpha < 0$) a bound state should exist *below* the continuum. Indeed, the condition $G_{1,1}^{-1}(k,\omega_b) = 0$ gives

$$z_b(\pi) = \frac{\Delta_1}{\alpha} - 1 + \frac{1}{\frac{\Delta_1}{\alpha} - 1} < -2. \tag{35}$$

For $k \neq \pi$, a bound state exists, too.[2] In Ref. 2, the isotropic version ($\Delta_1 = \Delta_2 = 1$) of the Hamiltonian (2) was considered. There, A. Chubukov has found that the dispersion of the two-magnon bound state $z_b(k)$ exhibits a minimum at $k = \pi$ for $|\alpha| > |\alpha_c| \approx 0.38$. The latter number will be refined below.

Based on extensive numerical work[5,6] for finite chains, and qualitative discussion in Ref. 3, we strongly believe that the two-particle bound state defined by (35) is the excitation with the *lowest* energy per flipped spin in the system for this parameter regime. The absolute dominance of two-magnon states manifests itself by $\Delta S^z = 2$ steps of the calculated magnetization curves $M(H)$ at high fields. Only for $\alpha \lesssim 0.4$ steps with $\Delta S^z = 3$ are observed (see Fig. 1 of Ref. 6). But we admit that from a formal point of view, the full rigorous solution should also include the analysis of the problem for the arbitrarily n-magnon bound states ($n \geqslant 3$) in a similar way as done here. However, the corresponding calculations are rather cumbersome and particular examples ($n = 3, 4$) are left for future consideration.

Then the quantum saturation field is determined by the condition that the two-magnon energy vanishes (i.e., the two-magnon instability of the field-induced ferromagnetic ground state). This way, the central result of the present work yields

$$\omega_b(\pi, B_s) = 2\mu(B - B_s) = J_2^{xy} z_b(\pi) + 2\omega_0 = 0, \tag{36}$$

or

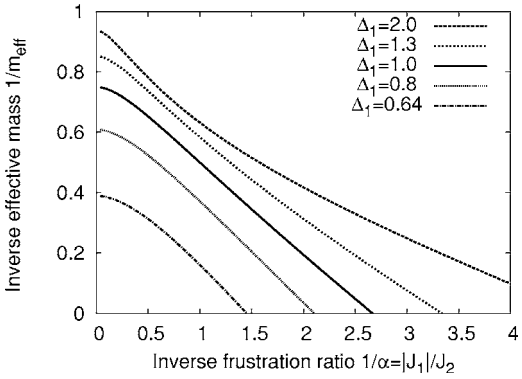

FIG. 1. The inverse effective mass (39) as a function of frustration ratio and anisotropy $\Delta_1 = J_1^z/J_1^{xy}$ for the $J_1 - J_2$ model.

$$\mu B_s = \frac{1}{2}\sum_r J_r^z - J_2^{xy} z_b(\pi), \tag{36'}$$

which gives explicitly

$$B_s = \frac{2J_2^{xy}(J_2^z + J_2^{xy}) - (J_1^z)^2 - 2J_2^z J_1^z}{2\mu(J_2^{xy} - J_1^z)}$$
$$= \frac{J_2^{xy}}{2\mu}\left[\frac{2(\Delta_2 + 1) - (\Delta_1/\alpha)^2 - 2\Delta_1/\alpha}{1 - \Delta_1/\alpha}\right]. \tag{37}$$

For the isotropic case, this result was first obtained in Ref. 2 by solving an integral equation which results from a summation of a sequence of ladder diagrams. From our straightforward derivation it is clear that the result is exact within the adopted two-magnon approach, as also pointed out in Ref. 3.

In order to find the parameter range where the value of $z_b(\pi)$ [see Eq. (35)] yields the minimum of the bound-state dispersion $z_b(k)$, we consider the expressions (25)–(27) in the vicinity of $k = \pi$, $z = z_b(k)$. After straightforward calculations given in the Appendix we obtain

$$z_b(k) \approx z_b(\pi) + \frac{(k - \pi)^2}{2m_{\text{eff}}}, \tag{38}$$

where

$$\frac{1}{2m_{\text{eff}}(\alpha,\Delta_1,\Delta_2)} = \frac{1}{2} + \frac{\Delta_1 - \alpha}{4\alpha\Delta_1^2} + \alpha\frac{\alpha - 2\Delta_1}{2(\alpha - \Delta_1)^2}$$
$$- \frac{(2\alpha - \Delta_1)\Delta_2}{4\Delta_1(\alpha - \Delta_1)[\alpha(1 + \Delta_2) - \Delta_1]}. \tag{39}$$

The dependence of the right-hand side of Eq. (39) on the inverse frustration ratio $|J_1/J_2|$ is shown in Fig. 1 for different values of the nearest-neighbor exchange anisotropy Δ_1. The dependence on the second-neighbor exchange anisotropy is weak in the vicinity of the isotropic point $\Delta_2 = 1$. We see that m_{eff} is positive for large values of frustration $J_2 \gg |J_1|$ and changes the sign at some critical value α_c, where the dispersion minimum is transformed to a local maximum. For $\Delta_2 = 1$ the condition $1/2m_{\text{eff}}(\alpha_c, \Delta_1, 1) = 0$ reduces to a cubic equation for α_c and we have

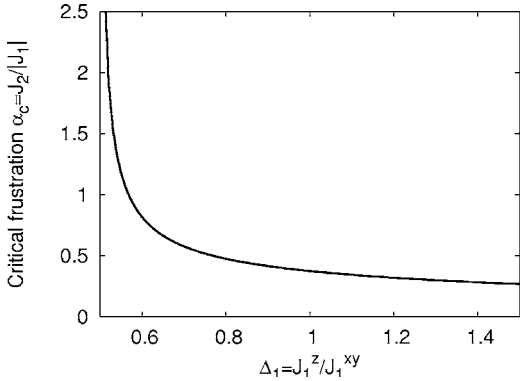

FIG. 2. The dependence of the frustration ratio value α_c, for which the effective mass (39) changes the sign, on anisotropy $\Delta_1=J_1^z/J_1^{xy}$ for the J_1-J_2 model.

$$\alpha_c(\Delta_1)=\Delta_1\left\{\frac{2}{3}-2R(\Delta_1)\cos\left[\frac{\phi(\Delta_1)+2\pi}{3}\right]\right\}, \quad (40)$$

where

$$R(\Delta_1)\equiv-\frac{1}{3}\sqrt{2\frac{5\Delta_1^2+1}{4\Delta_1^2-1}}, \quad \phi(\Delta_1)\equiv\arccos\left(-\frac{7}{54R^3}\right).$$

The critical frustration dependence on anisotropy is shown on Fig. 2. In the isotropic case, we have $R(1)=-2/3$, $\phi(1)=\arccos(7/16)$, and

$$\alpha_c(1)=\frac{2}{3}\left(2\cos\frac{\phi(1)+2\pi}{3}+1\right)\approx-0.374\,661\,059\,835\,27, \quad (41)$$

which refines $|\alpha_c(1)|\approx0.38$ calculated before.[2,3] If $\Delta_1\to0.5$, then α_c from Eq. (40) diverges, i.e., the effective mass $m_{\text{eff}}(\Delta_1=0.5)$ becomes negative for all frustration values.

Figure 3 shows the quantum and classical saturation field dependencies on the parameter values of the 1D isotropic J_1-J_2 model. We have chosen J_2 as the unit of energy. We see that the quantum effect is most pronounced for frustration values $|J_2/J_1|\sim1$.

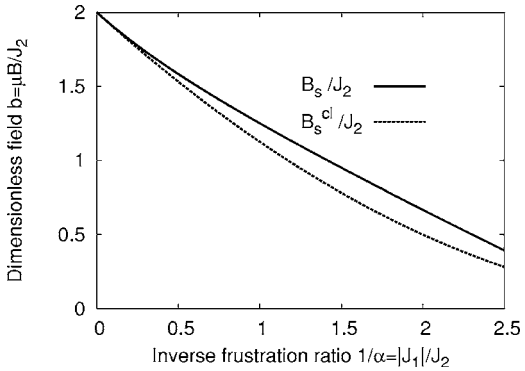

FIG. 3. The two-particle ($\mu B_{s,2}/J_2$—solid line) and one-particle ($\mu B_{s,2}^{\text{cl}}/J_2$—dashed line) values of the saturation field as a function of frustration ratio $|J_1|/J_2$ for the isotropic J_1-J_2 model.

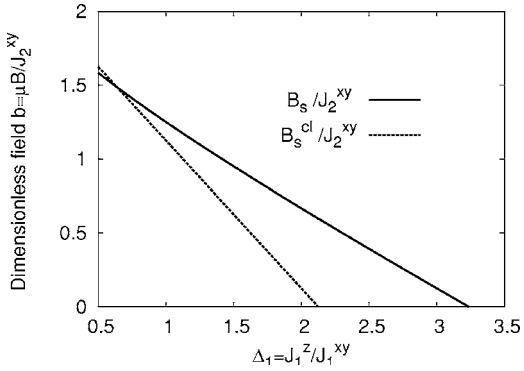

FIG. 4. The two-particle ($\mu B_{s,2}/J_2$—solid line) and one-particle ($\mu B_{s,2}^{\text{cl}}/J_2$—dashed line) saturation fields for the anisotropic J_1-J_2 model, $J_1=J_2=\Delta_2=1$.

In the region $0.25<|\alpha|<|\alpha_c|$ the minimum $z_b(k)$ for the isotropic model shifts into the point[2] $k=2q_0=2\arccos(-1/4\alpha)$. The authors of Ref. 3 argue that in this case the saturation field is determined by bound states of three and/or more magnons;[3] such a situation is out of the scope of this paper. For the anisotropic J_1-J_2 model, there is a third possible scenario. The one- and two-particle instabilities occur at different k points. Then, it is possible to have the minimum of $z_b(k)$ at $k=\pi$, which is higher in energy than the lowest boundary of the continuum (28) $z_c(2q_0)=z_c(2q_0)$. This happens, e.g., for the easy-plane nearest-neighbor anisotropy values

$$\Delta_1<\Delta_{1,a}=\frac{1+\sqrt{1+16\alpha^2}}{8|\alpha|}, \quad \Delta_2=1.$$

In Fig. 4 the dependence of the saturation fields on the anisotropy of the J_1 exchange is shown. The former is important for edge-shared cuprates.[7] We see that for $\Delta_1=(1+\sqrt{17})/8\approx0.640\,39$ the lines $B_s(\Delta_1)$ and $B_s^{\text{cl}}(\Delta_1)$ do intersect. At the same time $1/2m_{\text{eff}}(1,0.640\,39,1)\approx0.161\,78>0$. The unexpected at first glance result that the classical curve apparently reaches, then overwhelms the quantum result can be explained by the reduced attractive ferromagnetic interaction due to the anisotropy, i.e., a weakening of the two-magnon "glue." Below this value of Δ_1 the saturation field is determined by the one-particle instability, like in the XY model ($\Delta_1=\Delta_2=0$). Thus, the intersection is not related to a strange quantum versus classical behavior, but to the competition between one- and two-particle instabilities.

It is interesting that a strong easy-axis anisotropy can diminish the saturation field, and at the point

$$\Delta_{1,0}=(-\alpha)[1+\sqrt{3+2\Delta_2}]$$

the field B_s vanishes, i.e., the system's ground state becomes ferromagnetic.[2] Note also the region

$$\Delta_{1,0}^{\mathrm{cl}} = (-\alpha)\left[1 + \Delta_2 + \frac{1}{8\alpha^2}\right] < \Delta_1 < \Delta_{1,0},$$

where $B_s^{\mathrm{cl}}=0$, $B_s \neq 0$. Here the classical fully polarized state is destroyed by quantum fluctuations. A possible ground state for the system in this parameter regime may be a collinear state with period 4 described in Ref. 3, or a dimer nematic state, predicted in Ref. 2 for the isotropic model in a high field.

VI. ADDITIONAL INTERACTIONS

An advantage of our approach is the possibility to apply it to more complex situations which occur naturally when real chain compounds are considered. Indeed, it is easy to realize that the exact mapping of the two-magnon problem onto the effective tight-binding Hamiltonian (21) is not restricted to 1D and to the J_1-J_2 model. We may generalize the Hamiltonian $\hat{H}$ (6) including into summation over r more distant neighbors in chain direction. This will introduce additional impurities and hoppings in the effective Hamiltonian (21). Moreover, we may consider also 2D or 3D systems. Then, the site indices m as well as r in (7) and (8) become vectors with corresponding changes in the effective Hamiltonian (21). It is straightforward to obtain the TMGF (23), but the expression becomes cumbersome. Here we will apply our general approach to answer the question how is the quantum effect for the saturation field in the J_1-J_2 model modified by some additional interactions often present in real compounds.

First, we include a small third-neighbor in-chain interaction J_3. Such a term may appear as a result of the spin-phonon interaction in the antiadiabatic regime, when the exchange constants $J_i \ll \hbar\omega_{\mathrm{ph}}$, the characteristic phonon frequencies, and the spin-phonon interaction is strong.[9] It is expected to be small $J_3 \ll |J_1|, J_2$ and antiferromagnetic.[8,9] Below, the subscript 2(3) refers to the J_1-J_2 and the $J_1-J_2-J_3$ model, respectively. In this section, for the sake of simplicity we give only formulas for the isotropic case $J=J^z=J^{xy}$. The minimum of the one-magnon spectrum (14) gives the value of the helicoidal wave vector and the classical value of the saturation field

$$\cos q_{0,3} = \frac{-J_2 + \sqrt{J_2^2 - 3J_3(J_1 - 3J_3)}}{6J_3}, \tag{42}$$

$$\approx \cos q_{0,2}\left(1 - \frac{3J_3}{J_1}\right), \tag{43}$$

$$B_{s,3}^{\mathrm{cl}} \approx B_{s,2}^{\mathrm{cl}} + \frac{J_3}{\mu}\left(1 - \frac{3}{4\alpha} + \frac{1}{16\alpha^3}\right); \tag{44}$$

we recall that $\alpha<0$.

The two-magnon Green's function (33) has the form

$$G_{1,1}(\pi,\omega) = \left[\omega - (2\omega_0 + J_1 - J_2) - \frac{J_2^2}{\omega - (2\omega_0 + J_3) - J_2\tau\left(\dfrac{\omega - 2\omega_0}{J_2}\right)}\right]^{-1}. \tag{45}$$

For small J_3 values, the bound-state energy and the saturation field varies linearly with J_3

$$\omega_{b,3} \approx \omega_{b,2} - J_3\left[\frac{\alpha(2-\alpha)}{(1-\alpha)^4} + 1\right],$$

$$B_{s,3} \approx B_{s,2} + \frac{J_3}{2\mu}\left[1 + \frac{\alpha(2-\alpha)}{(1-\alpha)^4}\right], \tag{46}$$

where the values $\omega_{b,2}$, and $B_{s,2}$ are given by Eq. (37). The slope of $B_{s,3}^{\mathrm{cl}}$ dependence on J_3 is larger than for $B_{s,3}$. It means, that positive J_3 suppress the quantum effect. The difference of saturation fields in quantum and classical cases becomes smaller.

As the simplest example for a two-dimensional system we consider a 2D set of chains parallel to the x axis coupled in perpendicular direction with the strength $J_\perp$. Then the one-magnon dispersion becomes two dimensional:

$$\omega_{\mathbf{q},2\mathrm{D}}^{\mathrm{SW}} = \omega_{q_x,1\mathrm{D}}^{\mathrm{SW}} + J_\perp(\cos q_y a - 1). \tag{47}$$

From this expression one readily obtains

$$\mu B_{2\mathrm{D}}^{\mathrm{cl}} = \mu B_{1\mathrm{D}}^{\mathrm{cl}} + J_\perp + |J_\perp|, \tag{48}$$

i.e., in this approximation the ferromagnetic interchain interaction does not affect the saturation field, whereas in the antiferromagnetic case it is enhanced by $2J_\perp$. In general, such a correction is especially important near the quantum critical point for ferromagnet-helimagnet transition $\alpha \approx (4+9J_3/J_2)^{-1}$, where the 1D saturation field by definition vanishes. Equation (48) should be understood as a lower bound for the saturation field near the critical point. The account of quantum fluctuations will lead to slightly higher values of B_s according to Ref. 3.

For an arbitrary $\mathbf{k}$ point, the GF (23) is found from the solution of a system of three linear equations, but along the line $\mathbf{k}=(\pi/a, k_y)$ the system reduces to a single equation which gives

$$G_{1,1}(\mathbf{k},\omega) = \{[G_{1,1}^{(0)}(\mathbf{k},\omega)]^{-1} - J_1\}^{-1}, \tag{49}$$

where the two-dimensional spectrum (47) should be used in the expression for the noninteracting GF (26). The dispersion of the isolated pole and the two-particle continuum boundary are shown in Figs. 5 and 6. For small $J_\perp$ (Fig. 5) one observes a well-separated bound state. Here, the absolute minimum of the continuum occurs at $\mathbf{k}=(2q_0,0)$ and at $\mathbf{k}=(0,0)$ its energy $z_c=-2.45J_2$ exceeds the minimum of the bound-state dispersion given by $z_b(0,\pi)=-2.615\,76J_2$. For

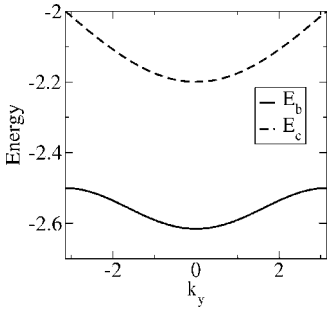

FIG. 5. The two-magnon bound-state energy $z_b(\pi,k_ya)=[\omega_b(\pi,k_ya)-2\omega_0]/J_2$ (solid line) and the boundary of the two-magnon continuum $z_c(\pi,k_ya)$ (dashed line) as a function of the quasimomentum value in the y direction for $|J_1|=J_2$; the interchain interaction is chosen as $J_\perp=0.1J_2$, J_2 being the unit of energy. For these parameters, the absolute minimum of continuum is $z_c(2q_0,k_ya)=-2.45J_2>z_b$.

strongly coupled chains such as $J_\perp=|J_1|=J_2$, the pole position becomes very shallow (Fig. 6) and it becomes clear that such a local minimum exceeds the minimum given by two independent (one-magnon) excitations ($z_c=-4.25J_2$ for the parameter set shown in the caption of Fig. 6). In the general 3D problem, one may expect that even the bound state itself may disappear.

At variance with the classical case given by Eq. (48), the solution of Eq. (49) yields for $|J_\perp|\ll J_2$

$$\mu B_s=\mu B_{s,1\mathrm{D}}+J_\perp+O(J_\perp^2/J_2), \tag{50}$$

i.e., in this case the saturation field is sensitive to both signs of the interchain interaction. With the increase of $J_\perp$ one finally reaches a critical value, where $z_b=z_c$ and beyond the "one-magnon" derived Eq. (48) should be used instead of a "two-magnon" one like Eq. (50). Thus, the quantum effects are maximally pronounced in the 1D case, just as the localization for the equivalent impurity problem. More complex interchain interactions derived from band structure calculations and inelastic neutron scattering data[10] and an application to chain cuprates will be given elsewhere.

VII. CONCLUSION

We have shown that the internal motion of a two-magnon pair on a ferromagnetic background is equivalent to the motion of a single particle described by an effective tight-binding Hamiltonian. This Hamiltonian is not translationally invariant. It models the hard-core boson constraint (5) by an infinite on-site energy at the site with zero coordinates, and each exchange $J_{\mathbf{r}}$ introduces the on-site energy $\varepsilon_{\mathbf{r}}$ and the hopping term $t_{\mathbf{r}}=J_{\mathbf{r}}\cos\mathbf{kr}/2$. Remarkably, this mapping procedure can be applied to problems at arbitrary dimension.

The two-magnon Green's function is found exactly by analogy with the impurity problem. The two-magnon excitation spectrum is found from poles and branch cuts of the Green's function. For the quasi-one-dimensional helimagnet with ferromagnetic nearest-neighbor and antiferromagnetic next-nearest-neighbor interactions a bound state of magnons exists. This leads to deviation of the quantum saturation field B_s from the classical value.

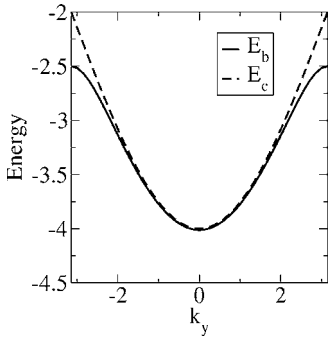

FIG. 6. The same as in Fig. 5 for $|J_1|=J_2=J_\perp$. The absolute minimum of the continuum is $z_c(2q_0,k_ya)=-4.25J_2<z_b$.

The derived expression for the saturation field B_s (exact within the two-magnon approach) provides a constraint for competing exchange interactions. Such a constraint may be useful in fitting thermodynamic properties such as the magnetic susceptibility $\chi(T)$ and the magnetic specific heat $c_p(T)$. In general, high-field magnetization measurements $M(H,T)$ yield important information concerning the exchange integrals in novel materials. Combined with the analysis of other experimental data, this knowledge may be very helpful to elucidate the relevant microscopic model of an acute-angle helimagnetic system (i.e., having a pitch angle $\leqslant\pi/2$ at zero magnetic field).

In this work we studied the lowest energy of excited states, i.e., the position of the isolated TMGF poles. The obtained Green's function (10) contains the information about the whole spectrum that is necessary for the calculations of physical properties for concrete materials. Various application to edge-shared compounds will be considered elsewhere.

ACKNOWLEDGMENTS

The authors thank the Heisenberg-Landau Program and the DFG (Project No. 436/UKR/17/8/05) for support. R.O.K. thanks the IFW Dresden, where the main part of this work has been carried out, for the hospitality. Discussions with V. Ya. Krivnov, D. V. Dmitriev, A. V. Chubukov, J. Richter, N. M. Plakida, and H. Eschrig are gratefully acknowledged.

APPENDIX: CALCULATIONAL DETAILS FOR THE "EFFECTIVE MASS" OF A MAGNON PAIR

Here we give details of the derivation of the Eqs. (38) and (39). The energy of an isolated pole of GF (25) is the root of the equation

$$-J_1^z+\frac{1}{G_{1,1}^{(0)}+\dfrac{G_{1,2}^{(0)}J_2^zG_{2,1}^{(0)}}{1-G_{2,2}^{(0)}J_2^z}}=0. \tag{A1}$$

It depends on k value via the dependence of hopping parameters t_r in $\hat{T}$ (21). We denote $\kappa\equiv\pi-k$, and expand the left-hand side of Eq. (A1) up to the terms $\propto\kappa^2$. Then

$$t_1 = J_1^{xy} \sin\frac{\kappa}{2} \approx J_1^{xy}\frac{\kappa}{2}, \quad t_2 = -J_2^{xy}\cos\kappa \approx -J_2^{xy}\left(1-\frac{\kappa^2}{2}\right).$$

Let us mention that the GF (27)

$$g_l(k,\omega) = g_{-l}(k,\omega) = \langle R|(\omega - \hat{T})^{-1}|R+l\rangle$$

obeys the equation of motion

$$(\omega - 2\omega_0)g_l = \delta_{l,0} + t_1(g_{l-1}+g_{l+1}) + t_2(g_{l-2}+g_{l+2}). \tag{A2}$$

We will calculate $g_0(k,\omega), g_1(k,\omega)$ directly from Eq. (27) and use (A2) for the calculation of other g_l involved in Eq. (A1). We begin with

$$g_0(k,\omega) = \frac{1}{2\pi}\int_{-\pi}^{\pi}\frac{dQ}{\omega - 2(\omega_0 + t_1\cos Q + t_2\cos 2Q)}. \tag{A3}$$

The denominator of the integrand is nonzero for the ω outside the spectrum of $\hat{T}$. After the substitution $\tau=\tan(Q/2)$ the straightforward calculations give

$$g_0 = -\frac{1}{8J_2^{xy}\cos\kappa\sqrt{(4q+p^2)(q+p-1)}} \times\left[\frac{p-2+\sqrt{4q+p^2}}{\sqrt{q+1-\sqrt{4q+p^2}}} - \frac{p-2-\sqrt{4q+p^2}}{\sqrt{q+1+\sqrt{4q+p^2}}}\right],$$

where

$$p \equiv -\frac{2\sin(\kappa/2)}{4\alpha\cos\kappa}, \quad q \equiv -\frac{z-2\cos\kappa}{4\cos\kappa}, \quad z \equiv \frac{\omega - 2\omega_0}{J_2^{xy}}.$$

Expanding this expression around the point $[k=\pi, z=z_b(\pi)]$, we obtain

$$g_0 \approx -\frac{1}{J_2^{xy}\sqrt{z^2-4}} \times\left[1-\kappa^2\left(1-\frac{\Delta_1}{\alpha}\right)^2\frac{4\Delta_1^2\alpha^2 - 3\alpha^2 + 3\Delta_1\alpha - \Delta_1^2}{2\Delta_1^3(2\alpha-\Delta_1)}\right]. \tag{A4}$$

In analogous way we obtain

$$g_1(k,\omega) = \frac{1}{2\pi}\int_{-\pi}^{\pi}\frac{\cos Q dQ}{\omega - 2(\omega_0 + t_1\cos Q + t_2\cos 2Q)} = -\frac{1}{2J_2^{xy}\sqrt{(4q+p^2)(q+p-1)}} \times\left[\frac{2q+p-\sqrt{4q+p^2}}{\sqrt{q+1-\sqrt{4q+p^2}}} - \frac{2q+p+\sqrt{4q+p^2}}{\sqrt{q+1+\sqrt{4q+p^2}}}\right] \approx \frac{\kappa\alpha}{2J_2^{xy}}\frac{(\alpha-\Delta_1)^2}{\Delta_1^3(2\alpha-\Delta_1)}. \tag{A5}$$

Now, using Eq. (A2), we have

$$g_2 + g_0 \approx \frac{1-\sqrt{\frac{z-2}{z+2}}}{2J_2^{xy}} \times\left[1-\kappa^2\frac{2\alpha\Delta_1^2(2\alpha^2 - 4\Delta_1\alpha + \Delta_1^2) - 3(\alpha-\Delta_1)^3}{4\Delta_1^4(2\alpha-\Delta_1)}\right]. \tag{A6}$$

Substituting the above expressions (A4)–(A6), into Eq. (26), we obtain

$$[G_{1,1}^{(0)}]^{-1} \approx \frac{2J_2^{xy}}{1-\sqrt{\frac{z-2}{z+2}}} \times\left\{1+\kappa^2\left[\frac{\alpha(2\alpha^2 - 4\Delta_1\alpha + \Delta_1^2)}{2\Delta_1^2(2\alpha-\Delta_1)} - \frac{(\alpha-\Delta_1)^3}{4\Delta_1^4(2\alpha-\Delta_1)}\right]\right\}, \tag{A7}$$

and

$$G_{1,2}^{(0)} = G_{2,1}^{(0)} \approx \frac{\kappa}{2J_2^{xy}}\frac{\alpha}{\Delta_1^2}, \tag{A8}$$

$$G_{2,2}^{(0)}(\pi, z_b(\pi)) \approx \frac{\alpha}{J_2^{xy}(\Delta_1 - \alpha)}. \tag{A9}$$

In the neighborhood of the point $k=\pi$, $z=z_b(\pi)$ Eq. (A1) may be rewritten as

$$-J_1^z + [G_{1,1}^{(0)}]^{-1} - \frac{[G_{1,2}^{(0)}]^2 J_2^z (J_1^z)^2}{1 - J_2^z G_{2,2}^{(0)}(\pi, z_b(\pi))} = 0.$$

The substitution of Eqs. (A7)–(A9), into this equation allows to solve it with respect to z and to obtain finally Eq. (38).

[1] C. Gerhardt, K.-H. Mütter, and H. Kröger, Phys. Rev. B **57**, 11504 (1998).
[2] A. V. Chubukov, Phys. Rev. B **44**, 4693 (1991).
[3] D. V. Dmitriev and V. Ya. Krivnov, Phys. Rev. B **73**, 024402 (2006).
[4] S.-L. Drechsler, N. Tristan, R. Klingeler, B. Büchner, J. Richter, J. Málek, O. Volkova, A. Vasiliev, M. Schmitt, A. Ormeci, C. Loison, W. Schnelle, and H. Rosner, J. Phys.: Condens. Matter (to be published); S.-L. Drechsler, J. Richter, R. Kuzian, J. Málek, N. Tristan, B. Büchner, A. S. Moskvin, A. A. Gippius, A.

Vasiliev, O. Volkova, A. Prokofiev, H. Rakoto, J.-M. Broto, W. Schnelle, M. Schmitt, A. Ormeci, C. Loison, and H. Rosner (unpublished).

[5] D. C. Cabra, A. Honecker, and P. Pujol, Eur. Phys. J. B **13**, 55 (2000).

[6] F. Heidrich-Meisner, A. Honecker, and T. Vekua, Phys. Rev. B **74**, 020403(R) (2006).

[7] V. Yu. Yushankhai and R. Hayn, Europhys. Lett. **47**, 116 (1999); S. Tornow, O. Entin-Wohlman, and A. Aharony, Phys. Rev. B **60**, 10 206 (1999); U. Ammerahl, B. Büchner, C. Kerpen, R. Gross, and A. Revcolevschi, *ibid.* **62**, R3592 (2000).

[8] S.-L. Drechsler, J. Richter, A. A. Gippius, A. Vasiliev, A. A. Bush, A. S. Moskvin, J. Málek, Yu. Prots, W. Schnelle, and H. Rosner, Europhys. Lett. **73**, 83 (2006); L. Capogna, M. Mayr, P. Horsch, M. Raichle, R. K. Kremer, M. Sofin, A. Maljuk, M. Jansen, and B. Keimer, Phys. Rev. B **71**, 140402(R) (2005).

[9] A. Weisse, G. Wellein, and H. Fehske, Phys. Rev. B **60**, 6566 (1999).

[10] M. Enderle, C. Mukherjee, B. Fåk, R. K. Kremer, J.-M. Broto, H. Rosner, S.-L. Drechsler, J. Richter, J. Málek, A. Prokofiev, W. Assmus, S. Pujol, J.-L. Raggazzoni, H. Rakoto, M. Rheinstädter, and H. M. Rønnow, Europhys. Lett. **70**, 237 (2005).